Erratum: New high-spin structure and possible chirality in ^{109}In [Phys. Rev. C 98, 014304 (2018)]

M. Wang, Y. Y. Wang, L. H. Zhu, B. H. Sun, G. L. Zhang, L. C. He, W. W. Qu, F. Wang, T. F. Wang, Y. Y. Chen, C. Xiong, J. Zhang, J. M. Zhang, Y. Zheng, C. Y. He, G. S. Li, J. L. Wang, X. G. Wu, S. H. Yao, C. B. Li, H. W. Li, S. P. Hu, and J. J. Liu

(Received 6 August 2020; published 14 December 2020)

DOI: 10.1103/PhysRevC.102.069903

In the original published paper the level energies were determined by the strongest transitions and other connecting γ-ray energies were deduced to be the difference between the initial and the final levels. In this Erratum, we modified the energies of all γ rays to their measured values and determine the level scheme by a simultaneous fit of all the γ-ray energies with weights for each γ ray determined by the error in its transition energy, properly taking into account any

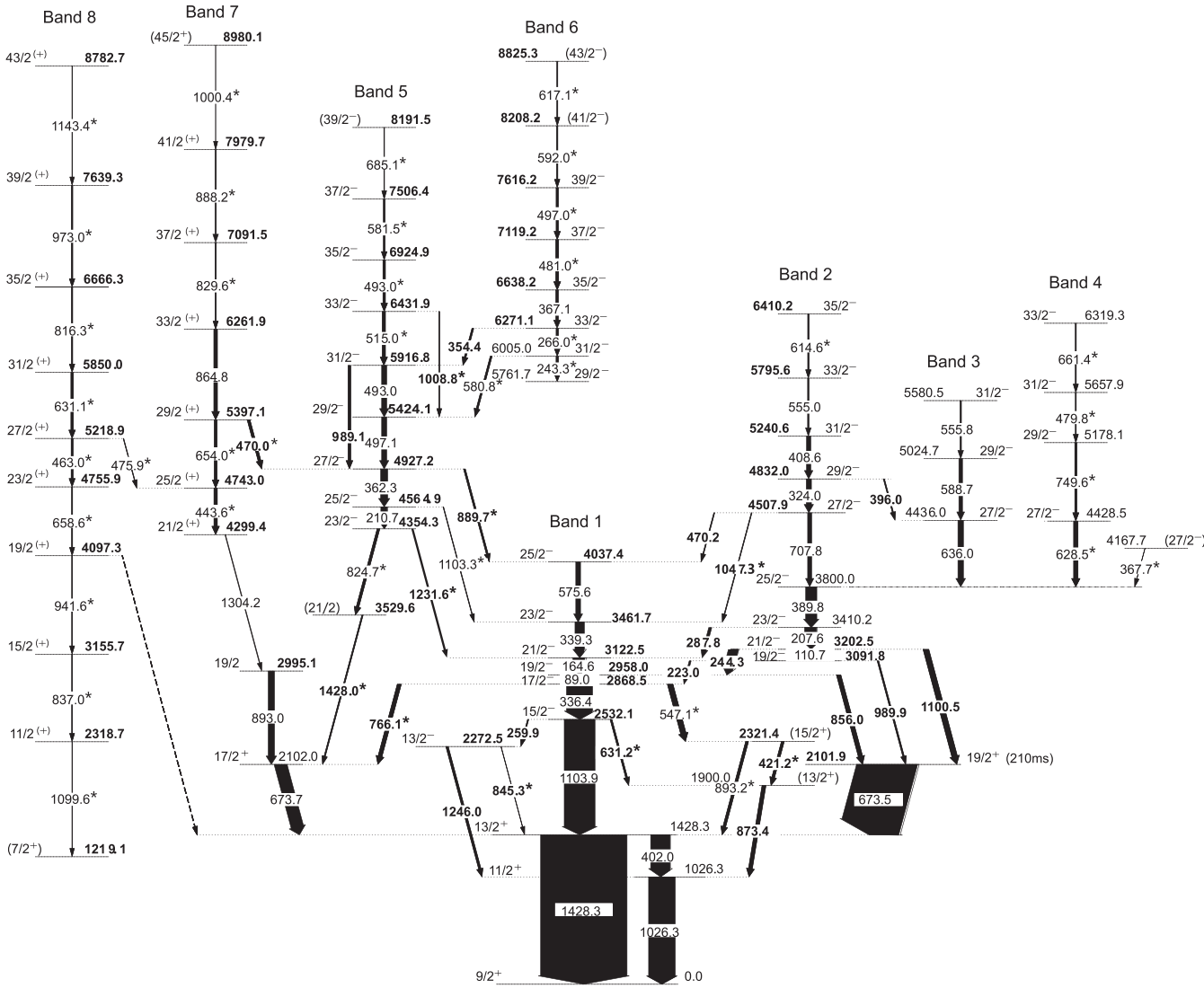

FIG. 1. Corrected level scheme of ^{109}In. The transitions marked with an asterisk(*) are newfound, and the energies which are updated in this Erratum are marked in bold.

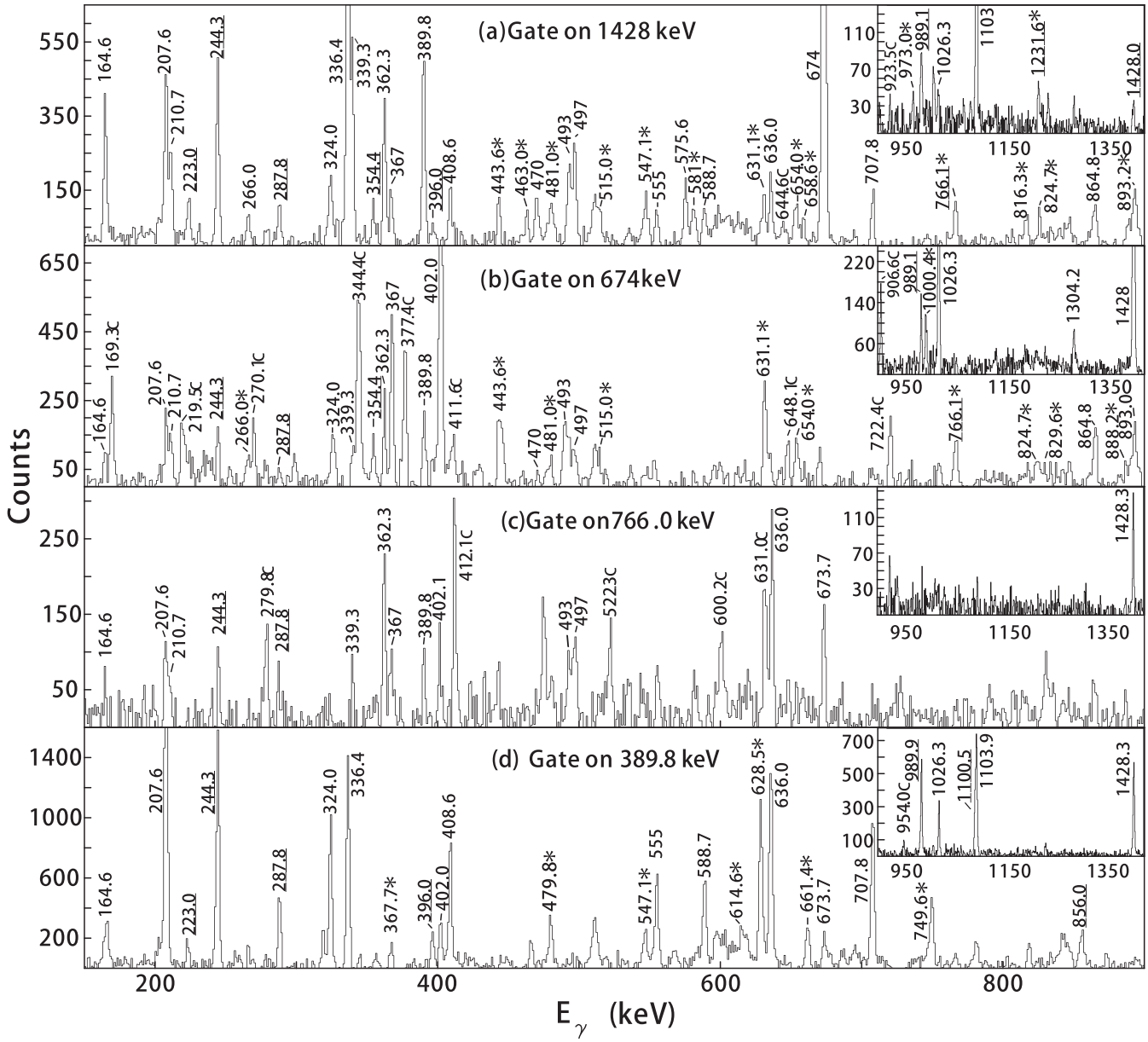

FIG. 2. γ-ray coincidence spectra with gates set on the (a) 1428-keV, (b) 674-keV, (c) 766.6-keV and (d) 389.8-keV transitions. The insets show the higher-energy part of the spectra. The energies marked by the asterisks are newly identified γ rays, and the energies marked by C are contaminants. The transitions for which the earlier energies are updated in this Erratum are marked by underlines.

coincidence information on placements. This Erratum, therefore, corrects the level scheme in Fig. 1, γ-ray coincidence spectra in Figs. 2–4, and Table I in the previously published paper by presenting new compilations with the actually measured γ-ray energies.

The changes from the published paper are in all cases small, and the physics conclusions arrived at previously are not changed.

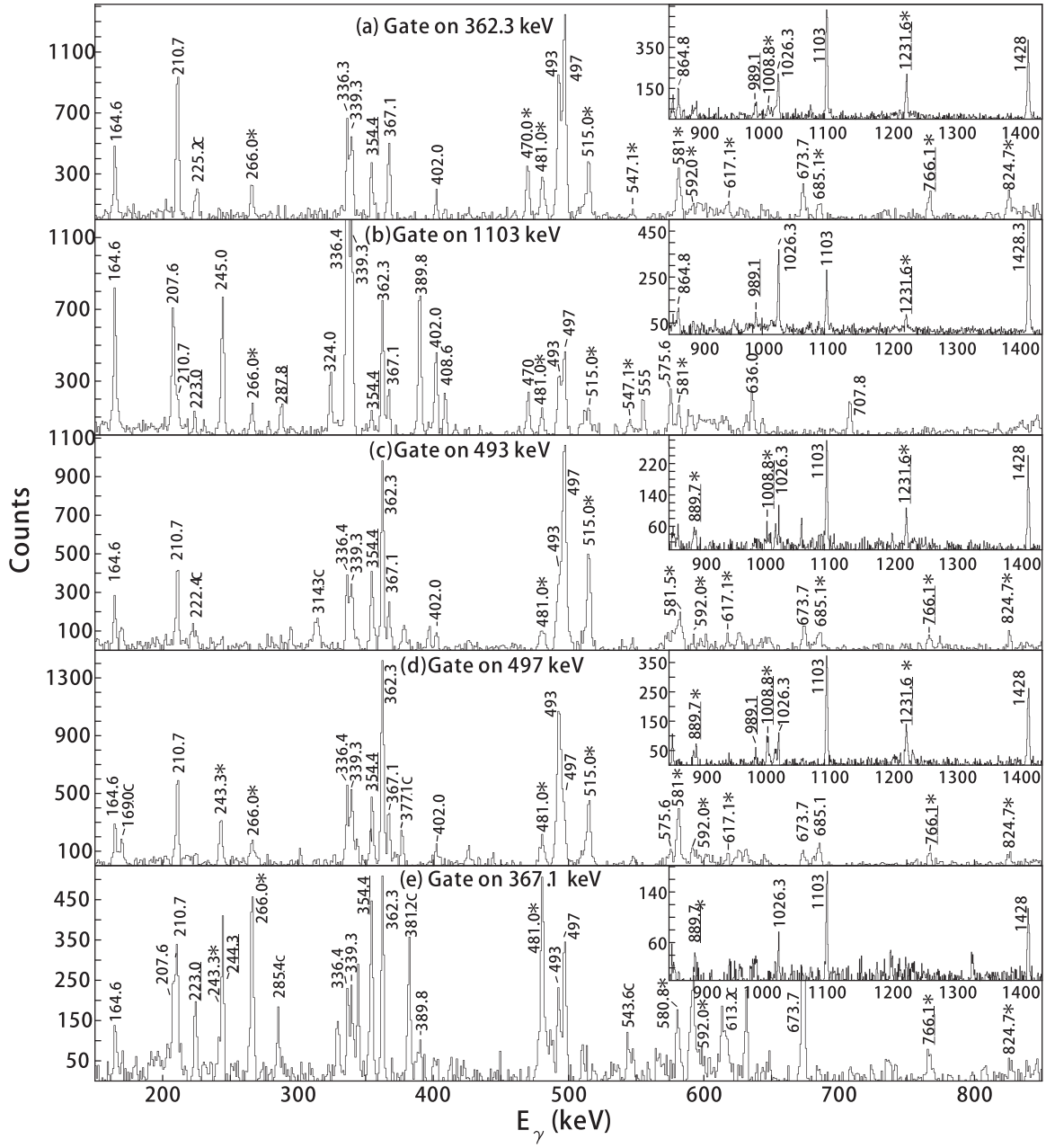

FIG. 3. γ-ray coincidence spectra with gates set on (a) 362.3-keV, (b) 1103-keV, (c) 493-keV, (d) 497-keV, and (e) 367.1-keV transitions. The insets show the higher-energy part of the spectra. The energies marked by the asterisks are newly identified γ rays, and the energies marked by C are contaminants.

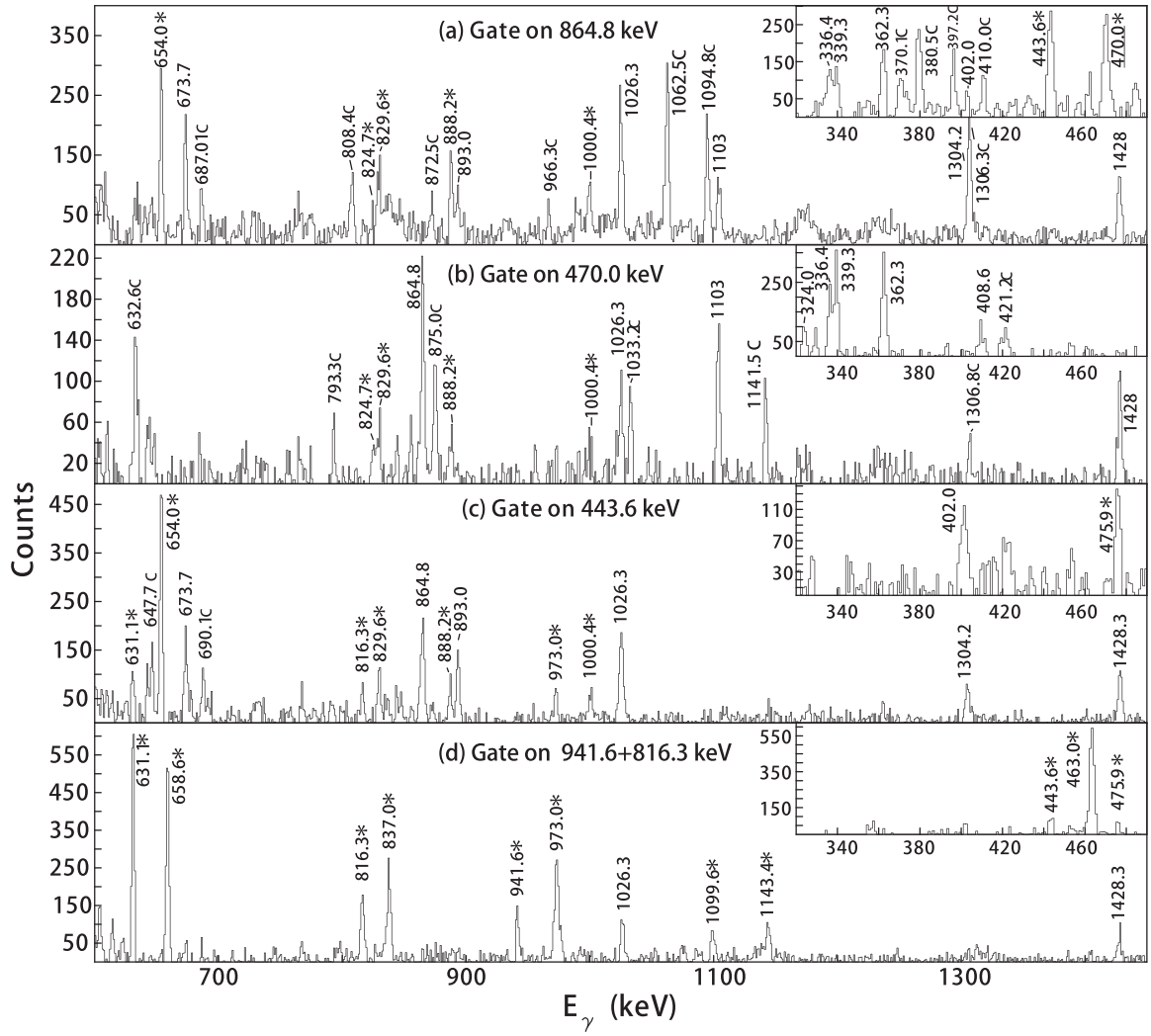

FIG. 4. γ-ray coincidence spectra with gates set on (a) 864.8 keV, (b) 469.7 keV, (c) 443.6 keV, and (d) 941.6+816.3 keV. The insets show the lower-energy part of the spectra. The energies marked by the asterisks are newly identified γ rays, and the energies marked by C are contaminants.

TABLE I. Corrected γ-ray energies, corrected initial and final level energies, intensities, DCO ratio, the initial and final level spin parities of ^{109}In.

E_γ (keV)[ae]	$E_i \rightarrow E_f$[e]	I_γ(%)[b]	$R_{\mathrm{DCO}}(D)$[c]	$R_{\mathrm{DCO}}(Q)$[d]	$I_i^\pi \rightarrow I_f^\pi$	Band
89.0	**2958.0** → **2868.5**	10(1)			$19/2^- \rightarrow 17/2^-$	
110.7	**3202.5** → **3091.8**	7(2)			$21/2^- \rightarrow 19/2^-$	2
164.6	**3122.5** → **2958.0**	38(2)	1.07(15)		$21/2^- \rightarrow 19/2^-$	1
207.6	3410.2 → **3202.5**	38(2)			$23/2^- \rightarrow 21/2^-$	2
210.7	**4564.9** → **4354.3**	20(1)			$25/2^- \rightarrow 23/2^-$	5
223.0	**3091.8** → **2868.5**	5.6(4)	1.18(30)		$19/2^- \rightarrow 17/2^-$	
243.3	6005.0 → 5761.7	7(1)	1.02(10)		$31/2^- \rightarrow 29/2^-$	6
244.3	**3202.5** → **2958.0**	31(1)	1.30(13)		$21/2^- \rightarrow 19/2^-$	2 → 1
259.9	**2532.1** → **2272.5**	3.9(6)			$15/2^- \rightarrow 13/2^-$	
266.0	**6271.1** → 6005.0	6.8(5)	1.17(13)		$33/2^- \rightarrow 31/2^-$	6
287.8	3410.2 → **3122.5**	9.2(6)	0.82(16)		$23/2^- \rightarrow 21/2^-$	2 → 1
324.0	**4832.0** → **4507.9**	16.2(9)	1.32(43)		$29/2^- \rightarrow 27/2^-$	2
336.4	**2868.5** → **2532.1**	82(3)	0.90(6)		$17/2^- \rightarrow 15/2^-$	
339.3	**3461.7** → **3122.5**	29(1)	1.09(8)		$23/2^- \rightarrow 21/2^-$	1
354.4	**6271.1** → **5916.8**	5.8(4)	1.05(13)		$33/2^- \rightarrow 31/2^-$	6 → 5
362.3	**4927.2** → **4564.9**	22(2)		1.05(14)	$27/2^- \rightarrow 25/2^-$	5
367.1	**6638.2** → **6271.1**	9(1)	0.99(14)		$35/2^- \rightarrow 33/2^-$	6
367.7	4167.7 → 3800.0	1(1)			$(27/2^-) \rightarrow 25/2^-$	
389.8	3800.0 → 3410.2	35(2)	1.06(15)		$25/2^- \rightarrow 23/2^-$	2
396.0	**4832.0** → 4436.0	3.8(3)			$29/2^- \rightarrow 27/2^-$	2 → 3
402.0	1428.3 → 1026.3	62(3)	0.61(17)		$13/2^+ \rightarrow 11/2^+$	
408.6	**5240.6** → **4832.0**	13.6(8)	1.14(11)		$31/2^- \rightarrow 29/2^-$	2
421.2	**2321.4** → 1900.0	9(3)	1.28(44)		$31/2^- \rightarrow 29/2^-$	
443.6	**4743.0** → **4299.4**	10.9(7)		0.82(17)	$25/2^{(+)} \rightarrow 21/2^{(+)}$	7
463.0	**5218.9** → **4755.9**	7.2(5)		1.07(16)	$27/2^{(+)} \rightarrow 23/2^{(+)}$	8
470.0	**5397.1** → **4927.2**	9(3)	0.64(8)		$29/2^{(+)} \rightarrow 27/2^-$	7 → 5
470.2	**4507.9** → **4037.4**	3(2)	1.20(31)		$27/2^- \rightarrow 25/2^-$	2 → 1
475.9	**5218.9** → **4743.0**	2(1)		0.60(10)	$27/2^{(+)} \rightarrow 25/2^{(+)}$	8 → 7
479.8	5657.9 → 5178.1	3(1)	0.81(17)		$31/2^- \rightarrow 29/2^-$	4
481.0	**7119.2** → **6638.2**	9(1)	0.85(7)		$37/2^- \rightarrow 35/2^-$	6
493.0	**5916.8** → **5424.1**	16.1(8)			$31/2^- \rightarrow 29/2^-$	5
493.0	**6924.9** → **6431.9**	8(1)			$35/2^- \rightarrow 33/2^-$	5
497.0	**7616.2** → **7119.2**	7(1)			$39/2^- \rightarrow 37/2^-$	6
497.1	**5424.1** → **4927.2**	16(2)			$29/2^- \rightarrow 27/2^-$	5
515.0	**6431.9** → **5916.8**	10.3(7)	0.54(8)		$33/2^- \rightarrow 31/2^-$	5
547.1	**2868.5** → **2321.4**	17.5(10)	0.90(17)		$17/2^- \rightarrow (15/2^+)$	
555.0	**5795.6** → **5240.6**	4.7(4)	1.10(14)		$33/2^- \rightarrow 31/2^-$	2
555.8	5580.5 → 5024.7	4.8(8)	0.85(20)		$31/2^- \rightarrow 29/2^-$	3
575.6	**4037.4** → **3461.7**	15.1(9)	0.90(7)		$25/2^- \rightarrow 23/2^-$	1
580.8	6005.0 → **5424.1**	6(1)	0.81(7)		$31/2^- \rightarrow 29/2^-$	6 → 5
581.5	**7506.4** → **6924.9**	5.0(10)	1.32(15)		$37/2^- \rightarrow 35/2^-$	5
588.7	5024.7 → 4436.0	11.6(7)	0.95(14)		$29/2^- \rightarrow 27/2^-$	3
592.0	**8208.2** → **7616.2**	4.4(4)			$(41/2^-) \rightarrow 39/2^-$	6
614.6	**6410.2** → **5795.6**	4.0(4)	0.58(10)		$35/2^- \rightarrow 33/2^-$	2
617.1	**8825.3** → **8208.2**	3(1)			$(43/2^-) \rightarrow (41/2^-)$	6
628.5	4428.5 → 3800.0	13.9(9)	0.70(7)		$27/2^- \rightarrow 25/2^-$	4 → 2
631.1	**5850.0** → **5218.9**	7.8(9)		1.04(11)	$31/2^{(+)} \rightarrow 27/2^{(+)}$	8
631.2	**2532.1** → 1900.0	6.0(9)			$15/2^- \rightarrow (13/2^+)$	
636.0	4436.0 → 3800.0	17.5(10)	0.69(5)		$27/2^- \rightarrow 25/2^-$	3 → 2
654.0	**5397.1** → **4743.0**	8.6(6)		0.83(10)	$29/2^{(+)} \rightarrow 25/2^{(+)}$	7
658.6	**4755.9** → **4097.3**	3.2(3)		0.93(9)	$23/2^{(+)} \rightarrow 19/2^{(+)}$	8
661.4	6319.3 → 5657.9	3.2(5)	0.59(32)		$33/2^- \rightarrow 31/2^-$	4
673.5	**2101.9** → 1428.3	188(7)			$19/2^+ \rightarrow 13/2^+$	
673.7	2102.0 → 1428.3	40(2)	1.62(23)		$17/2^+ \rightarrow 13/2^+$	
685.1	**8191.5** → **7506.4**	2.2(3)	0.71(33)		$(39/2^-) \rightarrow 37/2^-$	5
707.8	**4507.9** → 3800.0	12.8(8)	0.95(8)		$27/2^- \rightarrow 25/2^-$	2

TABLE I. (*Continued.*)

E_γ (keV)[ae]	$E_i \rightarrow E_f$[e]	I_γ(%)[b]	$R_{\rm DCO}(D)$[c]	$R_{\rm DCO}(Q)$[d]	$I_i^\pi \rightarrow I_f^\pi$	Band
749.6	5178.1 → 4428.5	6.5(5)	0.50(9)		$29/2^- \rightarrow 27/2^-$	4
766.1	**2868.5** → 2102.0	13.0(8)		1.45(35)	$17/2^- \rightarrow 17/2^+$	
816.3	**6666.3** → **5850.0**	4.1(4)		1.19(16)	$35/2^{(+)} \rightarrow 31/2^{(+)}$	8
824.7	**4354.3** → **3529.6**	8.5(6)	0.84(22)		$23/2^- \rightarrow (21/2)$	
829.6	**7091.5** → **6261.9**	3.2(5)		0.96(29)	$37/2^{(+)} \rightarrow 33/2^{(+)}$	7
837.0	**3155.7** → **2318.7**	2.7(7)		0.93(7)	$15/2^{(+)} \rightarrow 11/2^{(+)}$	8
845.3	**2272.5** → 1428.3	1(1)			$13/2^- \rightarrow 13/2^+$	
856.0	**2958.0** → **2101.9**	14(2)			$19/2^- \rightarrow 19/2^+$	
864.8	**6261.9** → **5397.1**	11.6(7)		0.80(7)	$33/2^{(+)} \rightarrow 29/2^{(+)}$	7
873.4	1900.0 → 1026.3	12.5(8)	1.16(36)		$(13/2^+) \rightarrow 11/2^+$	
888.2	**7979.7** → **7091.5**	4.3(6)		0.78(17)	$41/2^{(+)} \rightarrow 37/2^{(+)}$	7
889.7	**4927.2** → **4037.4**	5.9(5)			$27/2^- \rightarrow 25/2^-$	5 → 1
893.0	**2995.1** → 2102.0	20(2)		0.46(8)	$19/2 \rightarrow 17/2^+$	
893.2	**2321.4** → 1428.3	8(3)			$(15/2^+) \rightarrow 13/2^+$	
941.6	**4097.3** → **3155.7**	2.6(3)		1.10(13)	$19/2^{(+)} \rightarrow 15/2^{(+)}$	8
973.0	**7639.3** → **6666.3**	4.5(5)		0.98(13)	$39/2^{(+)} \rightarrow 35/2^{(+)}$	8
989.1	**5916.8** → **4927.2**	8.6(7)	1.30(41)		$31/2^- \rightarrow 27/2^-$	5
989.9	**3091.8** → **2101.9**	5.0(5)			$19/2^- \rightarrow 19/2^+$	
1000.4	**8980.1** → **7979.7**	0.4(3)			$(45/2^+) \rightarrow 41/2^{(+)}$	7
1008.8	**6431.9** → **5424.1**	2.6(3)			$33/2^- \rightarrow 29/2^-$	5
1026.3	1026.3 → 0	84(3)	0.59(7)		$11/2^+ \rightarrow 9/2^+$	
1047.3	**4507.9** → **3461.7**	2.4(3)			$27/2^- \rightarrow 23/2^-$	2 → 1
1099.6	**2318.7** → **1219.1**	1.3(2)			$11/2^{(+)} \rightarrow (7/2^+)$	8
1100.5	**3202.5** → **2101.9**	18(1)			$21/2^- \rightarrow 19/2^+$	
1103.3	**4564.9** → **3461.7**	2(2)			$25/2^- \rightarrow 23/2^-$	5 → 1
1103.9	**2532.1** → 1428.3	98(3)			$15/2^- \rightarrow 13/2^+$	
1143.4	**8782.7** → **7639.3**	1.2(6)		1.00(26)	$43/2^{(+)} \rightarrow 39/2^{(+)}$	8
1231.6	**4354.3** → **3122.5**	6.8(5)	0.51(12)		$23/2^- \rightarrow 21/2^-$	5 → 1
1246.0	**2272.5** → 1026.3	7.7(6)	0.57(25)		$13/2^- \rightarrow 11/2^+$	
1304.2	**4299.4** → **2995.1**	2.1(3)		0.54(11)	**4299.4** → **2995.1**	
1428.0	**3529.6** → 2102.0	4.1(5)			$(21/2) \rightarrow 17/2^+$	
1428.3	1428.3 → 0	273(16)			$13/2^+ \rightarrow 9/2^+$	

[a]Uncertainties are between 0.2 and 0.8 keV depending upon their intensity.
[b]Intensities are normalized to the doublet 1103-keV transitions with $I_\gamma = 100$.
[c]DCO ratios gated by dipole transitions.
[d]DCO ratios gated by quadrupole transitions.
[e]The energies which are updated in this Erratum are marked in bold.